



## Original article

## Multiple rapid-responsive probes for hypochlorite detection based on dioxetane luminophore derivatives

Yingai Sun <sup>a,1</sup>, Yuqi Gao <sup>b,1</sup>, Chunchao Tang <sup>a</sup>, Gaopan Dong <sup>a</sup>, Pei Zhao <sup>a</sup>, Dunquan Peng <sup>a</sup>, Tiantian Wang <sup>a</sup>, Lupei Du <sup>a</sup>, Minyong Li <sup>a,c,\*</sup><sup>a</sup> Department of Medicinal Chemistry, Key Laboratory of Chemical Biology (MOE), School of Pharmacy, Shandong University, Jinan, 250012, China<sup>b</sup> School of Pharmaceutical Sciences, Sun Yat-sen University, Guangzhou, 510006, China<sup>c</sup> State Key Laboratory of Microbial Technology, Shandong University, Jinan, 250100, China

## ARTICLE INFO

## Article history:

Received 26 December 2020

Received in revised form

21 September 2021

Accepted 8 October 2021

Available online 9 October 2021

## Keywords:

Glow-type

Chemiluminescent probe

1,2-Dioxetane

Hypochlorite

## ABSTRACT

In recent years, various methods for detecting exogenous and endogenous hypochlorite have been studied, considering its essential role as a biomolecule. However, the existing technologies still pose obstacles such as their invasiveness, high costs, and complicated operation. In the current study, we developed a glow-type chemiluminescent probe, hypochlorite chemiluminescence probe (HCCL)-1, based on the scaffold of Schaap's 1,2-dioxetane luminophores. To better explore the physiological and pathological functions of hypochlorite, we modified the luminophore scaffold of HCCL-1 to develop several probes, including HCCL-2, HCCL-3, and HCCL-4, which amplify the response signal of hypochlorite. By comparing the luminescent intensities of the four probes using the IVIS<sup>®</sup> system, we determined that HCCL-2 with a limit of detection of 0.166 μM has enhanced sensitivity and selectivity for tracking hypochlorite both in vitro and in vivo.

© 2021 The Authors. Published by Elsevier B.V. on behalf of Xi'an Jiaotong University. This is an open access article under the CC BY-NC-ND license (<http://creativecommons.org/licenses/by-nc-nd/4.0/>).

## 1. Introduction

Being an essential type of reactive oxygen species (ROS), hypochlorite is recognized as a significantly powerful antiseptic oxidant in the body. Superoxide anions are produced on the phagocytic lysosomal membrane of neutrophils; they then react with water to generate hydrogen peroxide [1], which subsequently oxidizes chloride ions to hypochlorite catalyzed by myeloperoxidase [2,3]. The formation of hypochlorite is part of the active defense against microorganisms, resulting from the ability of endogenous hypochlorite to cause exfoliation and death of endothelial cells in a concentration-dependent manner [4,5]. However, excess hypochlorite reacts with biomolecules rapidly under certain conditions, thus destroying the cellular structure and causing damage to healthy organs. Meanwhile, hypochlorite generates atherogenic lipoprotein granules that may induce cardiovascular disease,

neurodegenerative diseases, acute coronary syndrome, atherosclerosis, rheumatoid arthritis, lung injury, renal dysfunction, and even cancer [6–10]. Therefore, developing a method for detecting endogenous hypochlorite is necessary for diagnosing certain diseases and elucidating the basic process underlying the immune response.

To fully understand the pathophysiological significance of hypochlorite, numerous bioanalytical methods for hypochlorite detection have been developed, such as electrochemical analysis [11,12], chromatographic analysis [13,14], flow injection analysis [15,16], and potentiometry [17]. However, these conventional test methods have a common drawback. Real-time dynamic monitoring and in situ examination for detecting endogenous hypochlorite during biological activity are difficult to achieve, which significantly limits the applicability of these techniques.

Meanwhile, optical imaging has been recognized as a non-invasive, highly sensitive, and effective tool for detection in recent years [18–21], and a case in point is the fluorescence technique. In imaging hypochlorite, the fluorescent approach has been intensely developed to achieve visualization with high spatial and temporal resolution [22–24]. In 2016, Tang and coworkers [25] developed two fluorescent probes, *O*-(*N*-butyl-1,8-naphthalimide)-4-yl-*N,N*-dimethylthiocarbamate (NDMTC) and lyso-NDMTC, by

Peer review under responsibility of Xi'an Jiaotong University.

\* Corresponding author. Department of Medicinal Chemistry, Key Laboratory of Chemical Biology (MOE), School of Pharmacy, Shandong University, Jinan, 250012, China.

E-mail address: [mli@sdu.edu.cn](mailto:mli@sdu.edu.cn) (M. Li).

<sup>1</sup> Both authors contributed equally to this work.

<https://doi.org/10.1016/j.jpha.2021.10.001>

2095-1779/© 2021 The Authors. Published by Elsevier B.V. on behalf of Xi'an Jiaotong University. This is an open access article under the CC BY-NC-ND license (<http://creativecommons.org/licenses/by-nc-nd/4.0/>).

employing thiocarbamate as the recognition group for detecting hypochlorous acid (HClO), which sensitively visualizes HClO in cellulose and distinguishes malignant cells from normal cells in mice. However, fluorescence imaging is rarely applied in *in vivo* studies because of the inevitable need for external light irradiation and its low penetration ability.

Compared with the fluorescence technique, bioluminescence imaging presents an ideal signal-to-noise ratio with insignificant phototoxicity. In 2018, using the luciferase–luciferin bioluminescence system, our group explored a bioluminescent probe, 2-(6((dimethylcarbamothioyl)oxy)benzo[d]thiazol-2-yl)-4,5-dihydrothiazole-4-carboxylic acid for hypochlorite detection caged with the recognition group of thiocarbamate. This probe exhibited intense luminescence such that it could be used to monitor endogenous hypochlorite in a mouse inflammatory model [26]. Nevertheless, the application of the bioluminescence technique is extremely limited because of the necessity of gene expression or external addition of luciferase.

Chemiluminescence imaging (CLI) has gradually gained attention owing to its advantage over bioluminescence, including the lack of demand for transfected cells and transgenic animals. In 1987, Schaap et al. [27,28] first addressed trigger-activatable chemiluminescence based on the structure of a phenoxy adamantylidene 1,2-dioxetane scaffold as a luminophore, which was named Schaap's dioxetane. By using the recognition group as a phenolic substituent for Schaap's dioxetane system, the designed chemiluminescent probe may be triggered by enzymes or analytes, leading to the decomposition of the recognition group and formation of phenoxide dioxetane. Subsequently, the luminophore undergoes a chemically initiated electron exchange luminescence mechanism and triggers light emission [29]. Schaap's dioxetane chemiluminescent probe has significantly expanded the scope of imaging applications in living systems and may be utilized *in vivo* in wild-type organisms [30].

Therefore, we focused on glow-type trigger-activatable Schaap's 1,2-dioxetane as a CLI agent [31–41]. This luminophore is an excellent emitter in organic solvents, especially in dimethyl sulfoxide (DMSO), but its luminescence intensity is diminished under physiological conditions [42]. Since this defect impressively limits its scope of application, many efforts have been made to amplify the chemiluminescence signal [43]. Specific surfactants such as enhancer Emerald-II increase the luminescence signal by partially creating a hydrophobic environment in an aqueous solution [43,44]. However, considering the stability and toxicity of surfactants in biological samples, the results of CLI with surfactants must still be examined. Another solution for amplifying the signal is to improve the inherent luminescence ability by luminophore modification [33,40]. Shabat and coworkers [39] reported several ways to obtain better emissive luminophores by introducing substituents with electron-withdrawing acrylic and dicyanomethylchromone (DCMC) acceptors at the *ortho* and *para* positions of the phenolic group, respectively. Lippert and co-workers [45] demonstrated that another substitute acetoxyethyl ester at the *ortho* position of phenol exhibits satisfactory performance in cellular systems and animal models.

$\text{Cl}^+$  decomposed from HClO undergoes electrophilic addition to the sulfide moiety and specifically reacts with thiocarbamate [25]; therefore, we introduced thiocarbamate to Schaap's dioxetane to generate a hypochlorite chemiluminescence probe (HCCL). Based on the luminophore modification methods, we developed several hypochlorite chemiluminescent probes: HCCL-1, HCCL-2, HCCL-3, and HCCL-4, which masked thiocarbamate as the recognition group according to the interaction between chloride and sulfide moieties (Fig. 1). The probe HCCL-1 is Schaap's 1,2-dioxetane luminophore alone caged with the recognition group, while HCCL-2, -3, and -4 are conjugated with acrylic acid, acetoxyethyl

acrylate, and DCMC, respectively. All probes exhibited high stability under physiological conditions, significant sensitivity, and excellent selectivity for hypochlorite.

## 2. Experimental

### 2.1. Synthesis

The synthesis of probes HCCL-1, -2, -3, and -4 is described in Schemes S1–4. The detailed synthesis routes (Schemes S1–S4) and chemical characterizations (Figs. S1–S28) are presented in the Supplementary data.

### 2.2. Reagents

All solvents and chemicals purchased were used without further purification, if not specifically noted. Chemical reagents for the critical synthesis steps included 3-hydroxy benzaldehyde, tri(*o*-tolyl) phosphine (Heowns, Tianjin, China); benzoyl chloride (Guangfu, Tianjin, China); *n*-butyllithium, lithium diisopropylamide (Infinity Scientific, Beijing, China); 2-adamantanone, palladium acetate (Energy Chemical, Shanghai, China); and DABCO, bromomethyl acetate, and rose bengal (Aladdin, Shanghai, China).

Column chromatography filled with 200–300 mesh silica gel (Qingdao Haiyang Chemical Co., Ltd., Qingdao, China) was selected using ethyl acetate and petroleum ether as the eluent. Thin-layer chromatography on a silica gel plate was used to visualize the target product using ZF-2 UV254 ultraviolet light (Shanghai Baoshan Gucun Photoelectricity Instrument, Shanghai, China). Liquid chromatography/electrospray/high-resolution mass spectrometry-based chemical characterization was used to conduct mass spectral analysis (AB Sciex API 4000, Framingham, MA, USA). The  $^1\text{H}$  (400 MHz) and  $^{13}\text{C}$  (100 MHz) NMR spectra were recorded using a Bruker apparatus (Bruker, Karlsruhe, Germany). Chemical shifts ( $\delta$  values, ppm) and coupling constants (*J* values, Hz) were recorded in solvents of DMSO- $d_6$  and  $\text{CDCl}_3$  as the internal standards.

All biological solvents and reagents were used without further purification, unless otherwise specified. ROS such as sodium hypochlorite solution (Sinopharm Chemical Reagent Co., Ltd., Shanghai, China), potassium superoxide (Acros, Morris Plains, NJ, USA), hydrogen peroxide (30% (*m/m*), 9.97 M, Fuyu Chemical, Tianjin, China), di-*tert*-butyl peroxide (Aladdin, Shanghai, China), sodium nitrite (Aladdin, Shanghai, China), ferrous chloride (Guangfu, Tianjin, China), and acetic acid (Sinopharm Chemical Reagent Co., Ltd., Shanghai, China) were obtained commercially. Rabbit plasma was purchased from PingRuiBiotec (Henan Yiqi Biotechnology Co., Ltd., Zhengzhou, China). The water in the chemiluminescence studies was further purified using a Milli-Q filtration system (Millipore S.A.S., Molsheim, France).

### 2.3. Bioactivity evaluation apparatus

Chemiluminescence intensity signals were obtained using the IVIS<sup>®</sup> Kinetic Imaging System (Caliper Life Sciences, Hopkinton, MA, USA) equipped with a cooled charge-coupled device camera. Using the data processing software of the imaging system, the total flux of the photon emission per second ( $\text{p/s/cm}^2/\text{sr}$ ) in the selected region of interest was quantified.

### 2.4. Stability assay

Tris-HCl buffer (50 mM) with pH ranging from 3 to 10 was used to test the effect of pH on probe stability. Probes HCCL-1, -2, -3, and -4 were diluted to 100  $\mu\text{M}$  with Tris-HCl and incubated for 60 min

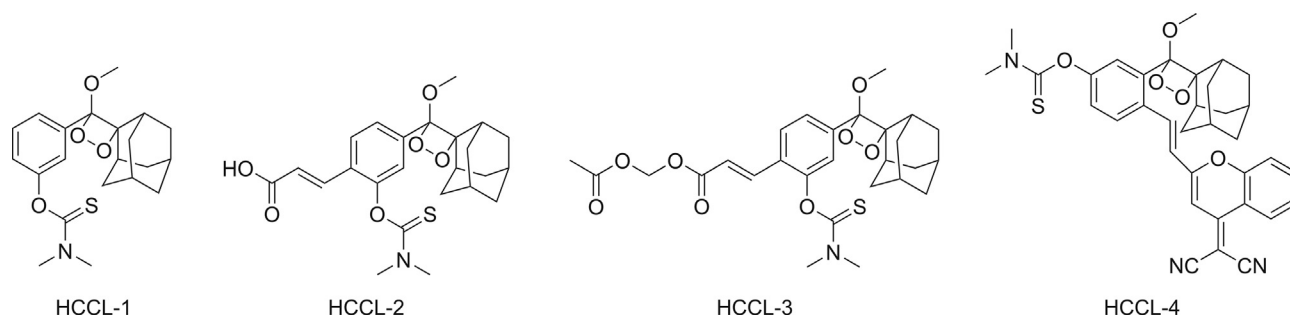


Fig. 1. Structures of probes hypochlorite chemiluminescence probe (HCCL)-1, HCCL-2, HCCL-3, and HCCL-4.

with Tris-HCl buffer at different pH values (3–10) at 37 °C. Chemiluminescence signals were then collected with an acquisition period of 60 s using the IVIS<sup>®</sup> Kinetic Imaging System.

### 2.5. Selectivity assay

Phosphate-buffered saline (PBS) buffer (1×, pH 7.4) was used for practical applications in biological systems to conduct selectivity measurements. Probes HCCL-1, -2, -3, and -4 at 100 μM were incubated with various 1-mM ROS at 37 °C for 60 min. Chemiluminescence signals were then captured immediately using the IVIS<sup>®</sup> Kinetic Imaging System with an acquisition period of 60 s.

### 2.6. Chemiluminescence study in vitro

Probes HCCL-1, -2, -3, and -4 at 100 μM were mixed with different concentrations of sodium hypochlorite solution (0–250 μM) in PBS buffer (1×, pH 7.4). Chemiluminescence signals were measured immediately using the IVIS<sup>®</sup> Kinetic Imaging System with an acquisition period of 60 s. Data were collected every 5 min.

### 2.7. Cytotoxicity assay

Using the standard cell counting kit (CCK)-8 assay, the cell viability of probes on RAW 264.7 cells was determined. RAW 264.7 cells (100 μL, 4 × 10<sup>4</sup> per well) were seeded in a 96-well microplate for 24 h in advance. Probes HCCL-1, -2, -3, and -4 at concentrations of 0–250 μM were added to a plate and co-incubated with the cells for 6 h. Optical density values were recorded.

### 2.8. Chemiluminescence study in cellulo

Macrophages may be stimulated by lipopolysaccharide (LPS) in cellulo, resulting in the production of endogenous hypochlorite [46]. In this study, RAW 264.7 cells were cultivated in Dulbecco's Modified Eagle Medium with 10% fetal bovine serum, and cell suspensions with 100 μL of 4 × 10<sup>4</sup> cells per well were seeded in a 96-well microplate at 37 °C for 24 h. Cells in plates were divided into three groups: blank, control, and experimental groups. LPS (100 μL, 5 μg/mL) was added to the cells in the experimental group and incubated for 4 h. Subsequently, 100 μL of PBS buffer (10 mM, pH 7.4) was added to the cells in the blank group, and 100 μL of 100-μM probes HCCL-1, -2, and -4 were added to the cells in the control and experimental groups. Immediately, chemiluminescence signals were measured with an acquisition period of 60 s using the IVIS<sup>®</sup> Kinetic Imaging System.

### 2.9. Chemiluminescence study in plasma

To confirm whether the probes were suitable for biological samples, a chemiluminescence assay was performed using rabbit plasma. Sodium hypochlorite solution was diluted with 10-fold diluted rabbit plasma to obtain different concentrations from 0 to 250 μM and mixed with 100 μM of probes HCCL-1, -2, -3, and -4. Chemiluminescence signals were measured immediately using the IVIS<sup>®</sup> Kinetic Imaging System with an acquisition period of 60 s. Data were acquired every 5 min.

### 2.10. Chemiluminescence study in vivo

The following animal studies were conducted with permission from the Institutional Animal Care and Use Committee and Ethics Committee of Cheeloo College of Medicine, Shandong University, and were implemented following the European guidance for the use of laboratory animals. Six BALB/c nude mice aged 4–5 weeks were purchased from the Animal Center of the China Academy of Medical Sciences (Beijing, China) to image endogenous hypochlorite in vivo. They were separated into two different groups, one of which was injected intraperitoneally (i.p.) with 1 mL of saline as the vehicle. The other group was administered 1 mL of 0.1 mg/mL LPS i.p. as the test group. After 4 h, all mice from both the vehicle and test groups were equally probed with 100 μL of 1 mM HCCL-2 via parenteral administration. Luminescence signals were recorded using the IVIS<sup>®</sup> Kinetic Imaging System with an acquisition period of 60 s, and data were acquired every 2 min.

## 3. Results and discussion

### 3.1. Chemiluminescence characteristics in vitro

All four probes had both thioamide bonds and thioester

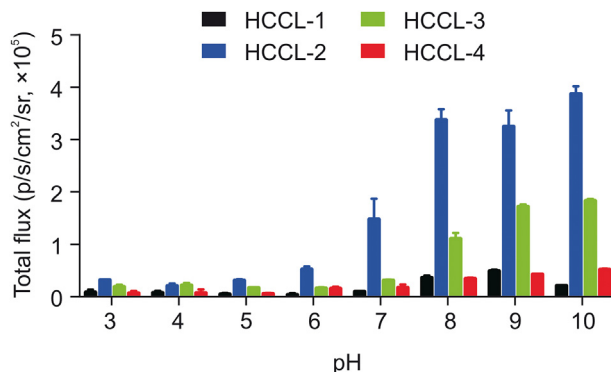
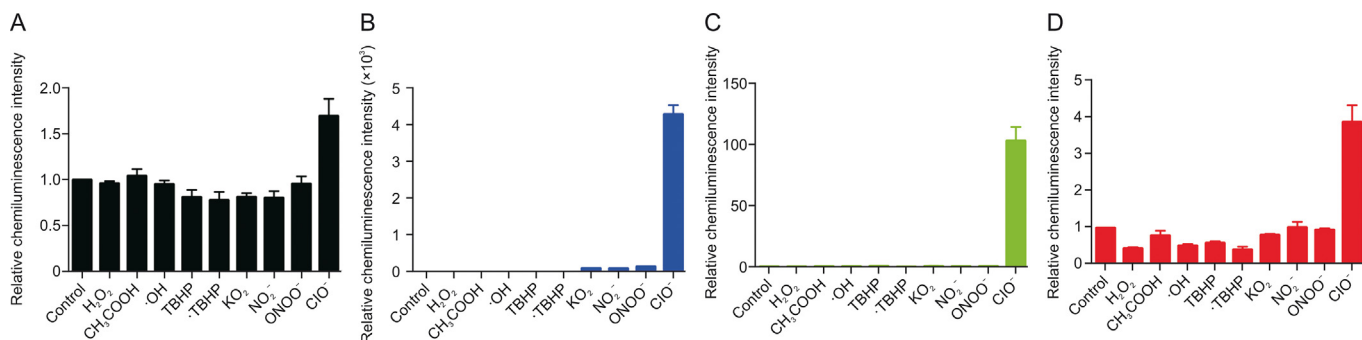


Fig. 2. Stability assays. Total chemiluminescence intensities of probes HCCL-1, -2, -3, and -4 (100 μM) in aqueous solutions of different pH values.



**Fig. 3.** Selectivity assays. Relative chemiluminescence intensities of (A) HCCL-1, (B) HCCL-2, (C) HCCL-3, and (D) HCCL-4 (100 μM) incubated with various reactive oxygen species.

structures. Therefore, it was necessary to validate their stability under different acidic and basic conditions to ensure that the probes could be applied at the physiological level. Based on the stability results, HCCL-1, -2, -3, and -4 were sufficiently stable under acidic and neutral conditions. This was because the probes showed less luminescence with pH values ranging from 3 to 7, which indicated that the probes maintained intact structures and less

decomposition into luminophores. Correspondingly, all probes were less stable under basic conditions in accordance with enhanced luminescence intensities (Fig. 2).

All probes indicated significant selectivity for hypochlorite among various types of ROS. The interaction between HCCL-2 and hypochlorite displayed 4200-fold higher chemiluminescence emission than that of the blank group, which was higher than those of HCCL-1, -3, and -4 with 1.7-, 100-, and 3.8-fold enhancements, respectively (Fig. 3). Therefore, our probes can accurately track hypochlorite without being affected by other ROS.

When the probes interacted with different concentrations of hypochlorite, the chemiluminescence intensities displayed a specific time-dependent pattern (Fig. S29). To determine the effect of various structural modifications on light emission, we set the incubation time of all probes and hypochlorite to 35 min.

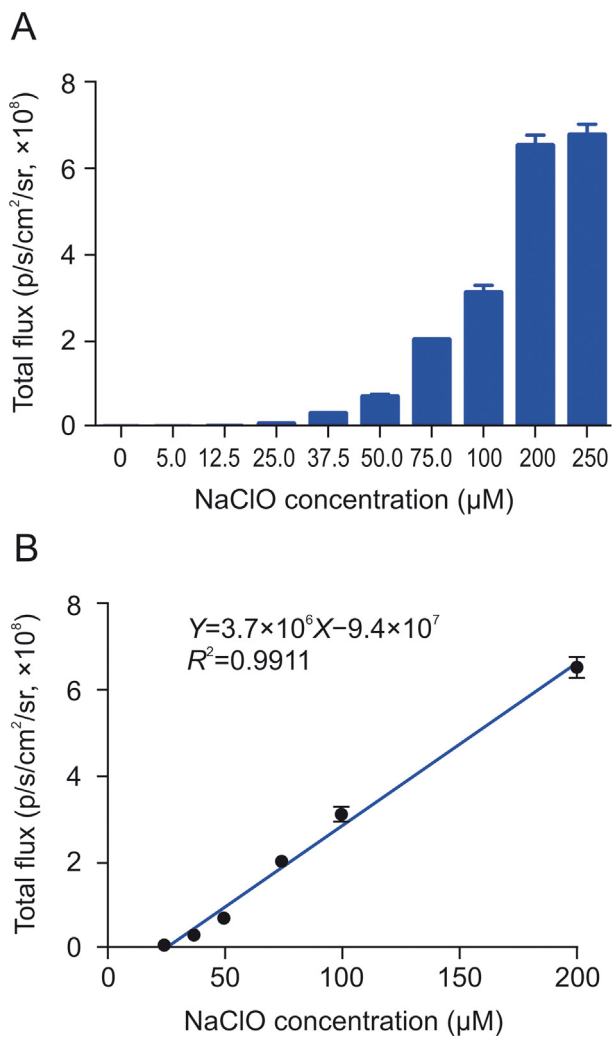


**Fig. 4.** (A) Chemiluminescence intensity of HCCL-2 (100 μM) with different concentrations of hypochlorite (0–250 μM) diluted with phosphate-buffered saline (PBS) (1×, pH 7.4) following incubation for 35 min. (B) Linear fit curve between the chemiluminescence intensity of HCCL-2 and various concentrations of hypochlorite.

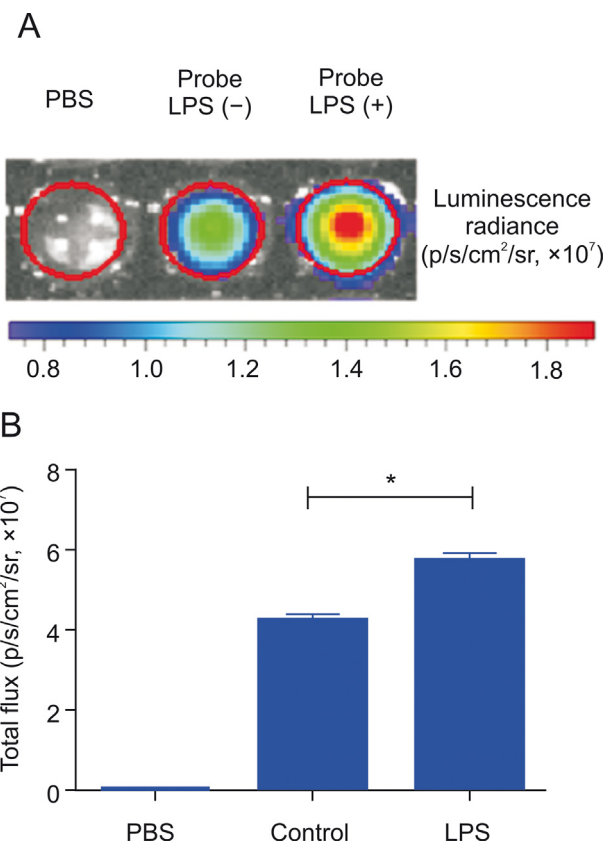


**Fig. 5.** Chemiluminescence imaging of HCCL-2 for endogenous hypochlorite in cellulo. (A) RAW 264.7 cells were cultivated with PBS, 100 μM of probe HCCL-2 or 5 μg/mL of LPS + 100 μM of probe HCCL-2. (B) Quantification of signal intensities of (A). \*P < 0.0001.

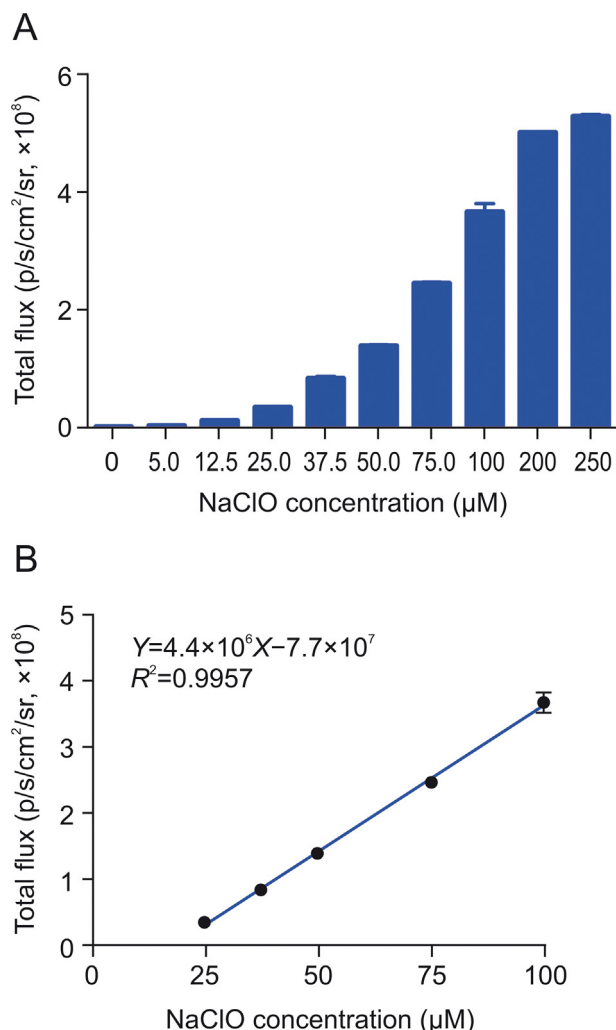


**Fig. 6.** (A) Chemiluminescence intensity of HCCL-2 (100 μM) with different concentrations of hypochlorite (0–250 μM) in 10-fold diluted rabbit plasma after 35 min of incubation. (B) Linear fit curve between the chemiluminescence intensity of HCCL-2 and various concentrations of hypochlorite.

The probe HCCL-2 presented high photon emission (6.8 × 10<sup>8</sup> p/s/cm<sup>2</sup>/sr) with 250 μM of sodium hypochlorite solution (Fig. 4A) and exhibited reliable linearity (Y = 3.7 × 10<sup>6</sup>X - 9.4 × 10<sup>7</sup>,

R<sup>2</sup> = 0.9911) at concentrations ranging from 25 to 200 μM of hypochlorite, and the limit of detection (LOD) was 0.166 μM (LOD = 3 × σ/slope) (Fig. 4B). Similarly, HCCL-1 presented a concentration-dependent pattern (Y = 2.1 × 10<sup>2</sup>X + 1.4 × 10<sup>4</sup>, R<sup>2</sup> = 0.9711) with an LOD of 25.882 μM, whereas HCCL-3 presented linearity (Y = 4.0 × 10<sup>3</sup>X + 2.7 × 10<sup>4</sup>, R<sup>2</sup> = 0.9908) with an LOD of 2.862 μM. HCCL-4 showed a dose-dependent pattern (Y = 82X + 1.6 × 10<sup>4</sup>, R<sup>2</sup> = 0.9246) with an LOD of 72.368 μM (Fig. S30). Considering the low LOD and strong chemiluminescence intensity, HCCL-2 was the most effective probe for detecting hypochlorite in vitro.

### 3.2. Chemiluminescence characteristics in cellulo

The CCK-8 assay was used to evaluate the cytotoxicity of the probes. As a result, the probe HCCL-3 exhibited high toxicity (half-maximal inhibitory concentration (IC<sub>50</sub>) < 38 μM) to cell lines in the experiment, which indicated the low biocompatibility of this probe (Fig. S31). Herein, chemiluminescence imaging of HCCL-1, -2, and -4 with low cytotoxicity (IC<sub>50</sub> > 1000 μM) in RAW 264.7 cells was performed to investigate the feasibility of tracking endogenous hypochlorite in cellulo.

Endogenous oxidant production, such as hypochlorite, may be induced by the stimulation of LPS in macrophages, followed by the activation of nicotinamide adenine dinucleotide phosphate oxidase [46]. In brief, the probe HCCL-2 generated the most intense chemiluminescence signal (5.8 × 10<sup>7</sup> p/s/cm<sup>2</sup>/sr) with prior LPS incubation. At 5 min, there was an obvious difference (P < 0.0001) between the LPS and control groups (Fig. 5B) and a significant signal difference in the real-time pseudo-color image (Fig. 5A). Correspondingly, HCCL-1 presented low intensity (9 × 10<sup>4</sup> p/s/cm<sup>2</sup>/sr) and a significant difference (P < 0.001) at 40 min, while HCCL-4 showed fair intensity (1.3 × 10<sup>5</sup> p/s/cm<sup>2</sup>/sr) and a significant difference (P < 0.001) at 60 min (Fig. S32). However, the real-time pseudo-color images used in the IVIS<sup>®</sup> Kinetic Imaging System minimally exposed the signal responses of HCCL-1 and HCCL-4 (Figs. S33A and C), presumably because of the low chemiluminescence intensity of the two probes, which was notably below the detection limit of the instrument. Therefore, the probe HCCL-2 determines endogenous hypochlorite in cellulo in real time.

### 3.3. Chemiluminescence characteristics in plasma

The luminescence activity of the probes in 10-fold diluted rabbit plasma was further tested, and the intensities revealed a specific time-dependent pattern that nearly reached the maximum values at

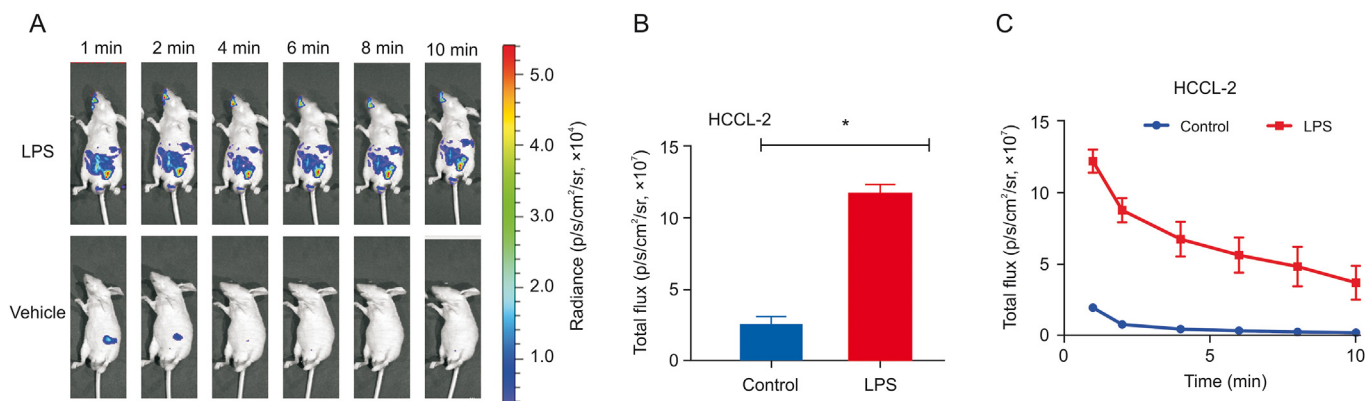


**Fig. 7.** Chemiluminescence imaging of HCCL-2 (1 mM) for endogenous hypochlorite. (A) Probe in nude mice via i.p. injection within 10 min. (B) Quantification of total photon flux. (C) Variation in chemiluminescence intensity within 10 min. \*P < 0.001.

35 min (Fig. S34). In the range of 25–100  $\mu\text{M}$  of hypochlorite, the chemiluminescence intensity of the probe HCCL-2 increased gradually and exhibited excellent linearity ( $Y = 4.4 \times 10^6 X - 7.7 \times 10^7$ ,  $R^2 = 0.9957$ ) with an LOD of 0.038  $\mu\text{M}$  (Fig. 6). Correspondingly, HCCL-1 fit a specific linear correlation ( $Y = 1.0 \times 10^3 X + 2.1 \times 10^5$ ,  $R^2 = 0.8837$ ) with an LOD of 29.667  $\mu\text{M}$ , whereas HCCL-3 exhibited reliable linearity ( $Y = 1.4 \times 10^5 X - 7.3 \times 10^5$ ,  $R^2 = 0.9913$ ) with an LOD of 0.289  $\mu\text{M}$ . HCCL-4 showed a concentration-dependent pattern ( $Y = 1.1 \times 10^3 X + 5.4 \times 10^4$ ,  $R^2 = 0.9881$ ) with an LOD of 21.856  $\mu\text{M}$  ranging from 25 to 100  $\mu\text{M}$  of hypochlorite (Fig. S35). Rabbit plasma was applied to simulate the internal environment of the organism, which demonstrated that the probes exhibited ideal biocompatibility. The results suggested that the probes were feasible for in vivo experiments.

### 3.4. Chemiluminescence characteristics in vivo

Based on the satisfactory performance of HCCL-2 in an aqueous solution and cell culture, the potential visualization capability of endogenous hypochlorite in vivo was subsequently investigated. As shown in Fig. 7A, HCCL-2 tracked endogenous hypochlorite within the organism. Compared with the vehicle-treated control group, the group injected with LPS showed a significant difference ( $P < 0.001$ ) at 1 min (Fig. 7B). The time-dependent pattern is shown in Fig. 7C. The probe HCCL-2 sensitively responded to endogenous hypochlorite and arrived at the peak value within 1 min, and the luminescent intensity then quickly decreased. At approximately 6 min, the signal decayed to half of its maximum value. In summary, the probe HCCL-2 may be used for the real-time detection and accurate imaging of in vivo hypochlorite.

## 4. Conclusions

This study developed new glow-type trigger-activatable chemiluminescent probes for hypochlorite imaging based on Schaap's 1,2-dioxetane derivatives. Using the "caged" strategy, HCCL-1, -2, -3, and -4 were designed and synthesized with specificity and high sensitivity via selection and in vitro assays. The probe HCCL-2 conjugated with acrylic acid presented an excellent signal response of endogenous hypochlorite with an LOD of 0.166  $\mu\text{M}$ . Moreover, the biocompatibility of HCCL-2 allowed for the tracking of endogenous hypochlorite in cellulo, exhibiting deep tissue penetration and high in vivo spatial resolution. Therefore, we anticipate that the best probe, HCCL-2, is a valuable tool for hypochlorite imaging and provides a powerful method for analyzing and detecting diseases involving hypochlorite. Moreover, the excellent performance of HCCL-2 in hypochlorite imaging also highlights the potential of Schaap's 1,2-dioxetane luminophores for chemiluminescence studies and applications.

### CRediT author statement

**Yingai Sun:** Conceptualization, Methodology, Validation, Formal analysis, Investigation, Writing - Original draft preparation, Reviewing and Editing; **Yuqi Gao:** Conceptualization, Methodology, Writing - Reviewing and Editing; **Chunchao Tang:** Conceptualization, Writing - Reviewing and Editing; **Gaopan Dong:** Conceptualization, Investigation, Writing - Reviewing and Editing; **Pei Zhao:** Investigation; **Dunquan Peng:** Investigation; **Tiantian Wang:** Investigation; **Lupei Du:** Conceptualization, Methodology, Formal analysis, Investigation, Resources, Supervision; **Minyong Li:** Conceptualization, Methodology, Formal analysis, Investigation, Resources, Supervision.

## Declaration of competing interest

The authors declare that there are no conflicts of interest.

## Acknowledgments

The present work was supported by grants from the National Natural Science Foundation of China (Grant Nos.: 81673393 and 81874308), Taishan Scholar Program in Shandong Province, and Shandong Natural Science Foundation (Grant No.: ZR2018ZC0233).

## Appendix A. Supplementary data

Supplementary data to this article can be found online at <https://doi.org/10.1016/j.jppha.2021.10.001>.

## References

- [1] S.J. Klebanoff, Myeloperoxidase: Friend and foe, *J. Leukoc. Biol.* 77 (2005) 598–625.
- [2] S. Gross, S.T. Gammon, B.L. Moss, et al., Bioluminescence imaging of myeloperoxidase activity in vivo, *Nat. Med.* 15 (2009) 455–461.
- [3] M.B. Hampton, A.J. Kettle, C.C. Winterbourn, Inside the neutrophil phagosome: Oxidants, Myeloperoxidase, and bacterial killing, *Blood* 92 (1998) 3007–3017.
- [4] Y.W. Yap, M. Whiteman, N.S. Cheung, Chlorinative stress: An under appreciated mediator of neurodegeneration? *Cell. Signal.* 19 (2007) 219–228.
- [5] S.J. Klebanoff, A.J. Kettle, H. Rosen, et al., Myeloperoxidase: a front-line defender against phagocytosed microorganisms, *J. Leukoc. Biol.* 93 (2013) 185–198.
- [6] M.J. Steinbeck, L.J. Nesti, P.F. Sharkey, et al., Myeloperoxidase and chlorinated peptides in osteoarthritis: Potential biomarkers of the disease, *J. Orthop. Res.* 25 (2007) 1128–1135.
- [7] D.I. Pattison, M.J. Davies, Evidence for rapid inter- and intramolecular chlorine transfer reactions of histamine and carnosine chloramines: Implications for the prevention of hypochlorous-acid-mediated damage, *Biochemistry* 45 (2006) 8152–8162.
- [8] A.M. Cantin, S.L. North, G.A. Fells, et al., Oxidant-mediated epithelial cell injury in idiopathic pulmonary fibrosis, *J. Clin. Invest.* 79 (1987) 1665–1673.
- [9] C.L. Hawkins, M.J. Davies, Degradation of hyaluronic acid, poly- and mono-saccharides, and model compounds by hypochlorite: Evidence for radical intermediates and fragmentation, *Free Radic. Biol. Med.* 24 (1998) 1396–1410.
- [10] E. Malle, T. Buch, H.J. Grone, Myeloperoxidase in kidney disease, *Kidney Int.* 64 (2003) 1956–1967.
- [11] O. Ordeig, R. Mas, J. Gonzalo, et al., Continuous detection of hypochlorous acid/hypochlorite for water quality monitoring and control, *Electroanalysis* 17 (2005) 1641–1648.
- [12] I. Seymour, B. O'Sullivan, P. Lovera, et al., Electrochemical detection of free-chlorine in water samples facilitated by *in-situ* pH control using interdigitated microelectrodes, *Sens. Actuators B Chem.* 325 (2020), 128774.
- [13] D.S. Jackson, D.F. Crockett, K.A. Wolnik, The indirect detection of bleach (sodium hypochlorite) in beverages as evidence of product tampering, *J. Forensic Sci.* 51 (2006) 827–831.
- [14] A. Gallina, P. Pastore, F. Magno, The use of nitrite ion in the chromatographic determination of large amounts of hypochlorite ion and of traces of chlorite and chlorate ions, *Analyst* 124 (1999) 1439–1442.
- [15] A. Chaurasia, K.K. Verma, Flow-injection spectrophotometric determination of residual free chlorine and chloramine, *Fresen. J. Anal. Chem.* 351 (1995) 335–337.
- [16] N.O. Soto, B. Horstkotte, J.G. March, et al., An environmental friendly method for the automatic determination of hypochlorite in commercial products using multisyringe flow injection analysis, *Anal. Chim. Acta* 611 (2008) 182–186.
- [17] A.P. Soldatkin, D.V. Gorchkov, C. Martelet, et al., New enzyme potentiometric sensor for hypochlorite species detection, *Sens. Actuators B Chem.* 43 (1997) 99–104.
- [18] T. Zhang, Y. Li, Z. Zheng, et al., *In situ* monitoring apoptosis process by a self-reporting photosensitizer, *J. Am. Chem. Soc.* 141 (2019) 5612–5616.
- [19] Y.L. Pak, S.J. Park, D. Wu, et al., N-Heterocyclic carbene boranes as reactive oxygen species-responsive materials: Application to the two-photon imaging of hypochlorous acid in living cells and tissues, *Angew. Chem. Int. Ed.* 57 (2018) 1567–1571.
- [20] M. Li, T. Xiong, J. Du, et al., Superoxide radical photogenerator with amplification effect: surmounting the Achilles' heels of photodynamic oncology, *J. Am. Chem. Soc.* 141 (2019) 2695–2702.
- [21] X. Liu, H. Lai, J. Peng, et al., Chromophore-modified highly selective ratiometric upconversion nanoprobes for detection of ONOO<sup>-</sup>-related hepatotoxicity in vivo, *Small* 15 (2019), 1902737.
- [22] R. Zhang, B. Song, J. Yuan, Bioanalytical methods for hypochlorous acid detection: recent advances and challenges, *TrAC Trends Anal. Chem.* 99 (2018) 1–33.

- [23] H. Xiao, K. Xin, H. Dou, et al., A fast-responsive mitochondria-targeted fluorescent probe detecting endogenous hypochlorite in living RAW 264.7 cells and nude mouse, *Chem. Commun. (Camb)* 51 (2015) 1442–1445.
- [24] Q. Xu, C.H. Heo, J.A. Kim, et al., A selective imidazoline-2-thione-bearing two-photon fluorescent probe for hypochlorous acid in mitochondria, *Anal. Chem.* 88 (2016) 6615–6620.
- [25] B. Zhu, P. Li, W. Shu, et al., Highly specific and ultrasensitive two-photon fluorescence imaging of native HOCl in lysosomes and tissues based on thiocarbamate derivatives, *Anal. Chem.* 88 (2016) 12532–12538.
- [26] C. Tang, Y. Gao, T. Liu, et al., Bioluminescent probe for detecting endogenous hypochlorite in living mice, *Org. Biomol. Chem.* 16 (2018) 645–651.
- [27] A.P. Schaap, T.S. Chen, R.S. Handley, et al., Cheminform abstract: Chemical and enzymatic triggering of 1,2-dioxetanes. Part 2. Fluoride-induced chemiluminescence from *tert*-butyldimethylsilyloxy-substituted dioxetanes, *ChemInform* 18 (1987) 1155–1158.
- [28] A.P. Schaap, M.D. Sandison, R.S. Handley, Cheminform abstract: Chemical and enzymatic triggering of 1,2-dioxetanes. Part 3. Alkaline phosphatase-catalyzed chemiluminescence from an aryl phosphate-substituted dioxetane, *ChemInform* 18 (1987) 1159–1162.
- [29] A.P. Schaap, T.S. Chen, R.S. Handley, et al., Chemical and enzymatic triggering of 1,2-dioxetanes. 2. Fluoride-induced chemiluminescence from *tert*-butyldimethylsilyloxy-substituted dioxetanes, *Tetrahedron Lett.* 28 (1987) 1155–1158.
- [30] N. Hananya, D. Shabat, A glowing trajectory between bio- and chemiluminescence: From luciferin-based probes to triggerable dioxetanes, *Angew. Chem. Int. Ed. Engl.* 56 (2017) 16454–16463.
- [31] M. Matsumoto, Advanced chemistry of dioxetane-based chemiluminescent substrates originating from bioluminescence, *J. Photoch. Photobio. C* 5 (2004) 27–53.
- [32] M. Matsumoto, N. Watanabe, N. Hoshiya, et al., Color modulation for intramolecular charge-transfer-induced chemiluminescence of 1,2-dioxetanes, *Chem. Rec.* 8 (2008) 213–228.
- [33] N. Hananya, D. Shabat, Recent advances and challenges in luminescent imaging: bright outlook for chemiluminescence of dioxetanes in water, *ACS Cent. Sci.* 5 (2019) 949–959.
- [34] I.S. Turan, E.U. Akkaya, Chemiluminescence sensing of fluoride ions using a self-immolative amplifier, *Org. Lett.* 16 (2014) 1680–1683.
- [35] J. Cao, R. Lopez, J.M. Thacker, et al., Chemiluminescent probes for imaging H<sub>2</sub>S in living animals, *Chem. Sci.* 6 (2015) 1979–1985.
- [36] J. Cao, J. Campbell, L. Liu, et al., In vivo chemiluminescent imaging agents for nitroreductase and tissue oxygenation, *Anal. Chem.* 88 (2016) 4995–5002.
- [37] I.S. Turan, O. Yilmaz, B. Karatas, et al., A sensitive and selective chemiluminogenic probe for palladium, *RSC Adv.* 5 (2015) 34535–34540.
- [38] I.S. Turan, O. Seven, S. Ayan, et al., Amplified chemiluminescence signal for sensing fluoride ions, *ACS Omega* 2 (2017) 3291–3295.
- [39] O. Green, S. Gnaim, R. Blau, et al., Near-infrared dioxetane luminophores with direct chemiluminescence emission mode, *J. Am. Chem. Soc.* 139 (2017) 13243–13248.
- [40] O. Green, T. Eilon, N. Hananya, et al., Opening a gateway for chemiluminescence cell imaging: Distinctive methodology for design of bright chemiluminescent dioxetane probes, *ACS Cent. Sci.* 3 (2017) 349–358.
- [41] N. Hananya, A.E. Boock, C.R. Bauer, et al., Remarkable enhancement of chemiluminescent signal by dioxetane-fluorophore conjugates: turn-ON chemiluminescence probes with color modulation for sensing and imaging, *J. Am. Chem. Soc.* 138 (2016) 13438–13446.
- [42] M. Matsumoto, Y. Mizoguchi, T. Motoyama, et al., Base-induced chemiluminescence of 5-*tert*-butyl-1-(4-hydroxybenz[d]oxazol-6-yl)-4,4-dimethyl-2,6,7-trioxabicyclo[3.2.0]heptanes: Chemiluminescence-chemiexcitation profile in aqueous medium, *Tetrahedron Lett.* 42 (2001) 8869–8872.
- [43] I. Bronstein, B. Edwards, J.C. Voyta, 1,2-Dioxetanes: Novel chemiluminescent enzyme substrates. Applications to immunoassays, *J. Biol. Chem.* 4 (1989) 99–111.
- [44] B. Gu, C. Dong, R. Shen, et al., Dioxetane-based chemiluminescent probe for fluoride ion-sensing in aqueous solution and living imaging, *Sens. Actuators B Chem.* 301 (2019), 127111.
- [45] L.S. Ryan, J. Gerberich, J. Cao, et al., Kinetics-based measurement of hypoxia in living cells and animals using an acetoxymethyl ester chemiluminescent probe, *ACS Sens.* 4 (2019) 1391–1398.
- [46] Y. Adachi, A.L. Kindzelskii, A.R. Petty, et al., IFN- $\gamma$  primes RAW264 macrophages and human monocytes for enhanced oxidant production in response to CpG DNA via metabolic signaling: roles of TLR9 and myeloperoxidase trafficking, *J. Immunol.* 176 (2006) 5033–5040.